Preprint
UCRL-JC-143446

Generating Low Temperature Layers with IR Heating

D.N. Bittner, G.W. Collins, and J.D. Sater

This article was submitted to Fusion Science and Technology

January 31, 2003

U.S. Department of Energy

Lawrence
Livermore
National
Laboratory

This work was performed under the auspices of the U.S. Department of Energy by the University of California, Lawrence Livermore National Laboratory under contract No. W-7405-Eng-48.

DISCLAIMER

UCRL-WEB-146893 Rev1-v4no1-03

Generating Low Temperature Layers with IR Heating

D.N. Bittner[1], G.W. Collins[2], and J.D. Sater[2]

[1] Schafer Corporation

303 Lindbergh Ave.

Livermore, CA 94551

[2] Lawrence Livermore National Laboratory

P.O. Box 808

Livermore, CA 94551

ABSTRACT

Cryogenic targets for the National Ignition Facility require uniform solid layers inside spherical capsules at temperatures approximately 1.5 K below the triple point of hydrogen. Uniform layers have been successfully formed near the triple point. However, upon subsequent cooling the layers degrade. We report here recent attempts to form uniform HD layers 1.5 K below the triple point using IR radiation. Pumping the IR collisionally induced vibration–rotation band of solid HD contained inside a transparent plastic shell generates a volumetric heat source in the HD lattice. This in turn allows the formation of a spherical crystalline shell of HD inside the transparent plastic shell. HD layers about 50 μm thick have been formed near the triple point and slowly cooled 1.5 K under high infrared power without layer degradation.

UCRL-WEB-146893 Rev1-v4no1-03

I. INTRODUCTION

Smooth and uniform 50 to 300 μm thick deuterium-tritium (D-T) layers on the interior of 1 to 3 mm diameter spherical capsules are required for ignitable inertial confinement fusion (ICF) targets for the National Ignition Facility (NIF)(1). One way to form these layers is to initially freeze D-T to an anisotropic multicrystalline solid inside a capsule and then allow the tritium decay volumetric heat generation, $Q_{D\text{-}T}$ = 0.05 W/cm^3, to symmetrize the layer. The volumetric heating causes the thicker regions of the solid to have a higher temperature and thus a higher vapor pressure. This results in a redistribution of the solid until the inner D-T surface is isothermal. The time constant for this redistribution (when no ^{3}He is present) is $\tau_O = H_s\rho/Q_{D-T}$ = 23 minutes, where H_s is the heat of sublimation (J/mole), and ρ is the density (moles/cm^3)(2). If bulk heating was the only factor controlling the layer profile, D-T would form a uniform spherical layer inside an isothermal spherical capsule. However, crystal surface stiffness contributes to the final layer shape. The surface structure of a multicrystalline D-T film is a function of the D-T bulk heating rate and the distribution of crystallite sizes and orientations which are determined by the initial nucleation and growth(3).

Several implosion hydrodynamics issues of cryogenic targets can be investigated with deuterium hydride (HD) or (deuterium) D_2 without the hazards of handling high pressure tritium. To generate bulk heat for mass redistribution without tritium radiation, we pumped the collisionally induced infrared (IR) vibration-rotation band. We controlled the solid volumetric heating rate, Q_{IR}, and thus the redistribution rate, $1/\tau_{IR}$, and surface roughness by controlling the incident IR intensity. The maximum Q_{IR} for hydrogen isotopes is limited by the vibrational relaxation time to $Q_{IR} \sim 1000 Q_{D\text{-}T}$(4). These large Q_{IR} values enabled us to control the hydrogen layer profile as well as to explore the redistribution process of laser heated solids.

UCRL-WEB-146893 Rev1-v4no1-03

We have previously reported on experiments where we generated a 4π illumination of HD inside a 1 mm O.D. spherical capsule and observed the evolution of a uniform solid layer as a function of time and IR intensity(5). Initial IR layering experiments formed layers from the solid. However, layers formed this way were extremely rough. In order to improve the quality of the inner solid surface, a second technique was developed. A solid HD sample was first illuminated with IR radiation and then slowly warmed until the solid melted. As soon as the solid melted the temperature was lowered until solid started reforming in the shell. At that point the sample temperature was held constant until the solidification process was complete. This process was developed using volumetric heating rates on the order of eight times the volumetric heating rate of D-T ($8Q_{D\text{-}T}$) on layers 150 μm or greater in thickness. Results were shown of a uniform and relatively thick HD layer formed just below the triple point of HD.

In the case of both the tritiated as well as non-tritiated hydrogen samples, smooth layers are formed near their respective triple points (6). This is however not the NIF design point temperature. Attempts to continue the slow cool process in D-T to 1.5 K below the triple point have not been successful. The layers tend to remain smooth to 0.5 – 0.8 K below the triple point at best before starting to degrade. We report here on the results of successful slow cooldown experiments conducted on HD samples illuminated with IR radiation at volumetric heating rates ranging from approximately $1Q_{D\text{-}T}$ to $50Q_{D\text{-}T}$.

II. EXPERIMENTAL DESIGN

A. EXPERIMENTAL DESIGN AND LAYOUT

Figure 1 contains a sketch of the experimental layout. For these experiments a 965 μm O.D. by 891 μm I.D. CD plasma polymer shell was placed in the center of a 25 mm I.D. integrating sphere. The fill line was composed of two sections: a 5 mm long tapered glass tube

UCRL-WEB-146893 Rev1-v4no1-03

attached to a 7.2 mm long stainless steel tube. The glass tube was 100 μm O.D. x 70 μm I.D. with one end drawn down to approximately 30 μm O.D. to fit into a 30 μm O.D. hole drilled into the shell. The glass tubing was epoxied into the shell and, after aligning the shell in the integrating sphere viewport, the other end of the tubing was epoxied into the stainless steel tube. The stainless tube extended through the integrating sphere wall. To minimize IR absorption in the fill line, the glass tube was coated with approximately 1000Å of gold. The laser used for these experiments was a mid-IR optical parameter oscillator (OPO) laser with an output power greater than 300 mW(7).

The integrating sphere was a vacuum tight enclosure made from aluminum with four window ports and an Infragold coating(8) on the inner surface. The Infragold surface is greater than 96% reflecting at wavelengths of interest. The diffuse reflections off the rough integrating sphere surface reduced laser induced coherence effects and produced a uniform 4π IR illumination at the capsule. The IR beam was coupled into an optical fiber at the laser output port to transport the IR into the integrating sphere. An SMA bulkhead feedthrough connected the fiber from the laser to the fiber inside the cryostat. An off-axis hole was drilled in the integrating sphere parallel to the capsule fill line but offset by 9.65 mm. One end of a polished optical fiber was positioned with the fiber tip flush to the integrating sphere surface. A leak tight epoxy seal on the outside of the integrating sphere sealed the fiber in place. Expanding from the fiber tip, the IR beam traversed the integrating sphere parallel to the shell fill line, but the fiber offset prevented the beam from hitting the capsule before it hit and diffusely scattered from the integrating sphere wall. The integrating sphere was thermally and mechanically attached to the cold tip of a helium flow cryostat. To cool the shell, roughly 1.5 Torr of helium exchange gas filled the integrating sphere. The helium pressure was set to a low value to prevent convection from adversely affecting the layer symmetry.

UCRL-WEB-146893 Rev1-v4no1-03

The layer was monitored along a viewing axis perpendicular to the capsule fill line by backlighting the capsule through one port and using a Questar microscope on the opposite port for viewing. Images were acquired periodically during layer formation and subsequent cooling using a Photometrics 1317 by 1035 array CCD camera attached to the microscope. Real time monitoring of the layer was done with a Cohu camera mounted on the microscope's auxillary port.

B. DATA COLLECTION AND ANALYSIS PROCEDURES

The first requirement was to relate injected IR laser power to power absorbed by the HD. To determine the bulk heating rate we measured the redistribution time constant, $\tau_{IR}(\underline{9})$. This was accomplished by filling the capsule with liquid HD, rapidly cooling to around 15 K to freeze the HD, and then turning on the IR and collecting images of the evolving layer with time. Typically the HD thickness was small near the top of the shell but grew exponentially with time to form a uniform layer. The layer thickness, h, was measured on each image, the results plotted as a function of time, t, and the data fit to an exponential curve of the form $h = a\text{-}be^{-t/c}$, where a, b, and c were fit parameters. The exponential time constant is related to the IR volumetric heating rate, Q_{IR}, by $\tau_{IR} = H_s\rho/Q_{IR}$. The IR power was measured by disconnecting the optical fiber at the cryostat feedthrough connector and attaching it to a power meter. For these experiments, approximately 6 mW of laser power available at the cryostat feedthrough resulted in a redistribution time in HD equal to the redistribution time in D–T. In other words, 6 mW corresponded to a volumetric heating rate of $1Q_{D\text{-}T}$. By adjusting the OPO laser's output power we could generate volumetric heating rates in the range of approximately $1Q_{D\text{-}T}$ to $50Q_{D\text{-}T}$.

The typical layering process involved injecting IR into the integrating sphere, raising the temperature of the capsule until the solid just finished melting and then slowly lowering the temperature in approximately 0.005 K steps until freezing onset occurred, at which point the

UCRL-WEB-146893 Rev1-v4no1-03

temperature was no longer lowered. If the solidification process appeared to stop, then the temperature was lowered in 0.005 K steps until the HD completely solidified. Typically the solidification process finished before the temperature was lowered 0.1 K below the melting point. Once the HD solidified, the temperature was lowered 1.5 K at a constant cooling rate in steps of either 0.020 K every three minutes (20mK/3min.) or 0.010 K every three minutes (10mK/3min.). While the temperature was lowered, images of the layer were captured and stored every 6 min.

Roughness of the inner solid surface was determined by performing a Fast Fourier Transform (FFT) analysis of the brightband in the stored CCD camera images. The brightband was produced by total internal reflection of light rays off the inner solid surface(10). Software has been developed which locates the brightband in the image(11). The resultant one-dimensional estimates of the solid thickness variations were Fourier transformed giving values for the power spectrum and rms of perturbations on the solid layer. Early surface roughness calculations located the position of the inner edge of the brightband to determine these values. Computer raytrace modeling has since shown that a better estimate of the power spectrum and rms value is made by locating the position of the center of the brightband(12). The data presented in this paper use the center of the brightband position relative to the outer edge of the capsule to fit Fourier modes 1 through 128. Due to the perturbation caused by the fill tube, the defect in the layer near the fill tube (~17% of the brightband) was excluded before the brightband analysis was performed.

III. RESULTS

The goal of these experiments was to determine if a uniform HD layer formed and maintained under constant IR illumination near the triple point of HD could be kept from degrading while slowly lowering the temperature 1.5 K. The determination of whether or not

UCRL-WEB-146893 Rev1-v4no1-03

the layer degraded was done by a combination of both qualitative and quantitative analyses of the images. The quantitative information from our images was acquired by FFT analysis of the brightband. If the layer starts to degrade then the rms value for that layer will increase. Since there is currently no quantitative analysis performed on the center of the images, we looked qualitatively for the growth of features as the layer cooled. Changes in features were regarded as the growth of defects and interpreted as layer degradation.

Figure 2 contains a plot of the surface roughness results from one of the slow cooldown experiments. The laser power was set to generate a volumetric heating rate of $10Q_{D\text{-}T}$ and the temperature was lowered in 20mK/3min. steps. The plot shows the rms values from the brightband FFT analysis of the images for modes 4 to 100 plotted versus temperature. If the surface roughness did not change with temperature the data points would fit along a flat line, as indicated by the solid line in the plot. As one can see in this data, the surface rms value slowly increases to about 10% by the time the temperature is lowered 0.8 K. Below this temperature the rms value starts to increase more rapidly and between 1.3 K and 1.55 K the brightband is too discontinuous for analysis with our software. After dropping by 1.57 K the temperature was no longer lowered but images were acquired for an additional 43 minutes. During this time, some annealing of the surface occurred and we were able to analyze the images acquired during the final 28 minutes. This annealing was typical of most of the experiments. However, there was never an indication that sufficient annealing would occur with time to decrease the rms value to the value measured after initial layer formation.

Figure 3 shows four of the images acquired during the cooldown. The first image was captured after initial layer formation ($\Delta T = T_{melt} - T = 0.09$ K). This is our reference image. During the subsequent cooldown we looked for changes relative to the reference image indicating that the layer was degrading. The next image ($\Delta T = 1.03$ K) does not show any

UCRL-WEB-146893 Rev1-v4no1-03

break in the brightband but features are starting to grow near the bottom of the capsule. The third image ($\Delta T = 1.55$ K), acquired at the next to the last 20 mK temperature step, shows more features near the bottom of the capsule and multiple discontinuities in the brightband. The discontinuities here were too great for analysis. The final image ($\Delta T = 1.57$ K) was acquired after the layer sat at constant temperature for 43 minutes. One can see that some annealing of the layer has occurred, and one of the discontinuities near the bottom of the capsule has disappeared. However, this last image still shows a layer qualitatively as well as quantitatively rougher than the image at the start of the cooling sequence.

At a cooling rate of 20mK/3min. we were not able to maintain the layer quality. We were able to minimize the degree of layer degradation by increasing the volumetric heating rate. Figure 4 contains a pair of images from both a low, ~$1.3Q_{D\text{-}T}$, and a high, ~$46Q_{D\text{-}T}$, volumetric heating rate. The layer cooled using the low heating rate shows significant layer degradation. In fact, the layer rms value increased rapidly as the layer was cooled. The rms value (modes 4 to 100) started at 0.6 μm but the layer became too rough to analyze by the time the temperature was lowered 0.2 K. On the other hand, the layer cooled using a high volumetric heating rate showed a much slower layer degradation rate and the rms value (0.47 μm for modes 4 to 100) did not significantly change until near the end of the cooling cycle when the layer had cooled over 1 K.

Based on the results of these measurements a second set of slow cooldown experiments was conducted at a cooling rate of 10mK/3min. At this cooling rate it now took 7.5 hours to lower the temperature 1.5 K. Using this slower cooling rate with a relatively high volumetric heating rate we were able to maintain the layer quality through the entire cooldown process. Figure 5 shows the images of a layer taken at the start and the end of a cooldown where the volumetric heating rate was about $34Q_{D\text{-}T}$. As one can see, there are no qualitative differences in

UCRL-WEB-146893 Rev1-v4no1-03

the two images. Quantitatively, there is no significant difference between the rms values of these two images. Figure 6 shows the power spectra for these two images. Only small variations appear between the mode amplitudes. The table insert lists the rms values for the first several mode ranges. Most of the power is in the first three modes. The difference in rms values between the high (ΔT = 0.1 K) and low (ΔT = 1.5 K) temperature modes is less than 11%. For this second set of slow cooldown experiments, the lowest volumetric heating rate at which the layer quality was maintained was ~$25Q_{D\text{-}T}$.

IV. CONCLUSIONS

We have demonstrated that it is possible to maintain the integrity of a uniform HD layer at 1.5 K below the triple point by slowly cooling down the layer under IR illumination. The best layers were formed under high IR power, corresponding to heating rates of at least $25Q_{D\text{-}T}$, with a cooling rate of 10mK/3min. Layers formed and cooled under low IR power and layers cooled at a rate of 20mK/3min. degraded before the temperature was lowered 1.5 K.

These were a series of experiments to determine the feasibility of the slow cooling concept. There should be a determination of the minimum volumetric heating rate and maximum cooling rate necessary to maintain the layer to 1.5 K below the triple point. Only two constant cooling rates were used. At a cooling rate of 10mK/3min. the cooling cycle took nearly eight hours to lower the layer temperature 1.5 K. It may be possible to cool the layer at a faster rate at the beginning of the cooling cycle and then cool at a slower rate near the end of the cooling cycle. Further parametric studies are needed to determine an optimal cooling protocol.

ACKNOWLEDGMENTS

UCRL-WEB-146893 Rev1-v4no1-03

The authors would like to thank J. Burmann and W. Unites for their technical assistance. This work was performed under the auspices of the U.S. Department of Energy under contract no. W-7405-Eng-48 and contract no. DE-AC03-01SF22260.

UCRL-WEB-146893 Rev1-v4no1-03

REFERENCES

1 J. Lindl, Phys. of Plasmas, V2, N11:3933-4024 (1995); E. M. Campbell, J. C. Browne, Science 271 130-132 (1996).

2 A. J. Martin, R. J. Simms, and R. B. Jacobs, J. Vac. Sci. Technol. A **6** (3), 1885 (1988); J. K. Hoffer and L. R. Foreman, Phys. Rev. Lett. 60, 1310 (1988); T. P. Bernat, E. R. Mapoles, and J. J. Sanchez, ICF Quarterly **1**, 57 (1991).

3 *Solids Far From Equilibrium* edited by C. Godreche, (Cambridge University Press., Cambridge, 1992). In this paper we ignore effects from ^{3}He born in the solid. The effects of ^{3}He cannot be ignored in D-T layers which have aged for longer than ~ a day.

4 C. Y. Kuo, R. J. Kerl, N. D. Patel, and C. K. N. Patel, Phys. Rev. Lett. **53**, 2575 (1984).

5 D.N. Bittner, G.W. Collins, E. Monsler, and S. Letts, "Forming Uniform HD Layers in Shells Using Infrared Radiation", Fusion Technol., **35**, 244 (1999)

6 D.N. Bittner, T.P. Bernat, J. Burmann, G. W. Collins, B. Kozioziemski, S. Letts, E.R. Mapoles, E. Monsler, J. Pipes, M. Saculla, J.D. Sater, W. Unites, "Forming Uniform Deuterium Hydride and Deuterium-Tritium Layers in Shells", ICF Quarterly **8**, 131 (1998)

7 Aculight Corporation, 11805 North Creek Parkway S., Bothell, WA 98011

8 Infragold™ is an electrochemically plated, diffuse, gold-metallic coating. For information contact Labsphere, North Sutton, NH 03260.

9 G.W. Collins, D.N. Bittner, E. Monsler, S. Letts, E.R. Mapoles, and T.P. Bernat, " Infra-Red Redistribution of D_2 and HD Layers for ICF" , J. Vac. Sci. Technol. A., vol. 14, p. 2897 (Sep/Oct, 1996)

10 The brightband is formed by total internal reflection off the inner solid surface and its position is determined by the refractive effects of the CD shell as well as the solid HD. The correlation of the inner ice surface with the brightband is discussed further in references 5 and 12.

UCRL-WEB-146893 Rev1-v4no1-03

11 G. W. Collins, E. R. Mapoles, J. Sanchez, R. Bell, W. Unites, J. Hoffer, L. Forman, and J. Simpson, "Solid Hydrogen Surfaces," ICF Quarterly 3, 81 (1993).

12 J.A. Koch, T.P. Bernat, G.W. Collins, B.A. Hammel, B.J. Kozioziemski, A.J. MacKinnon, J.D. Sater, D.N. Bittner, and Y.Lee, "Quantitative Analysis of Backlit Shadowgraphy as a Diagnostic of Hydrogen Ice Surface Quality for ICF Capsules", Fusion Technol., 38, 123 (July, 2000)

UCRL-WEB-146893 Rev1-v4no1-03

Figure 1 Experimental layout indicating the viewing axis and the IR fiber. The shaded area inside the integrating sphere represents the spread of the injected IR beam.

Figure 2 An example plot of the brightband analysis results for one of the 20mK/3min. cooling rate experiments. The volumetric heating rate was $10Q_{D\text{-}T}$. The rms value was calculated for modes 4 to 100. The solid line indicates the rms value for the layer if it does not degrade.

Figure 3 Corresponding images from the slow cooldown of the layer analyzed in Figure 2. Figure 3a shows the layer near the triple point ($\Delta T = 0.09$ K). Figure 3b shows the layer at $\Delta T = 1.03$ K where additional small features are evident inside the brightband. Breaks in the brightband are seen near the end of the cooling cycle ($\Delta T = 1.55$ K) in Figure 3c. Figure 3d shows some annealing of the brightband after sitting at 1.57 K for 43 minutes.

Figure 4 Images comparing layers formed and cooled at 20mK/3min. under low (4a and 4b) and high (4c and 4d) IR power. Figure 4a is an image of a layer formed with a volumetric heating rate of $\sim 1.3Q_{D\text{-}T}$ and Figure 4b is the same layer after cooling 1.5 K. In contrast, Figure 4c is an image of a layer formed at $\sim 46Q_{D\text{-}T}$ and Figure 4d is the same layer after cooling 1.5 K.

Figure 5 Images of a layer cooled at 10mK/3min. under a volumetric heating rate of $\sim 34Q_{D\text{-}T}$. Figure 5a shows the layer just below the triple point and Figure 5b shows the layer 1.5 K below the triple point.

Figure 6 Power spectra for the two images shown in Figure 5. The thick line is the power spectrum of the layer after formation ($\Delta T = 0.1$ K) and the thin line is the power spectrum of the layer after cooling 1.5K. The table insert lists the various mode range rms values for comparison.

UCRL-WEB-146893 Rev1-v4no1-03

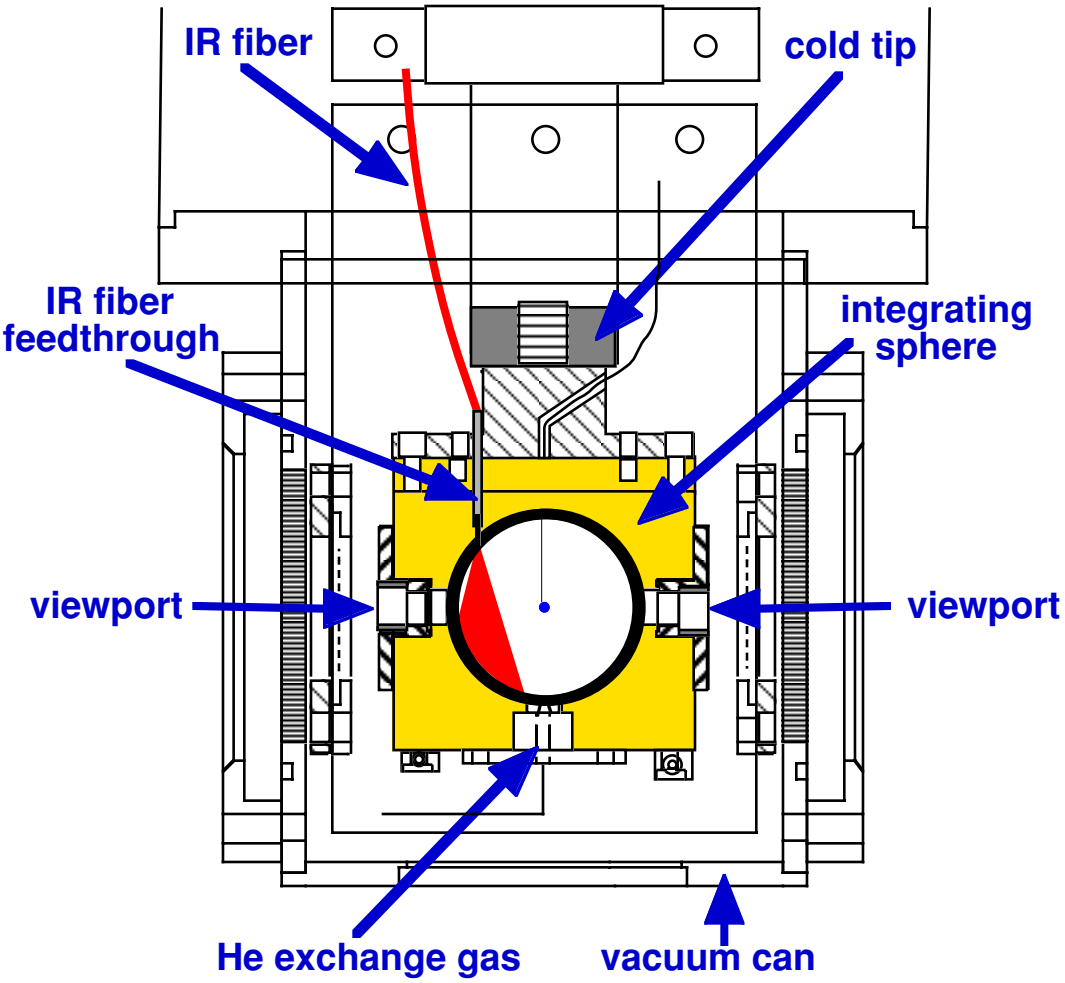

Generating Low Temperature Layers with IR Heating Figure 1

D.N. Bittner, G.W. Collins, and J.D. Sater

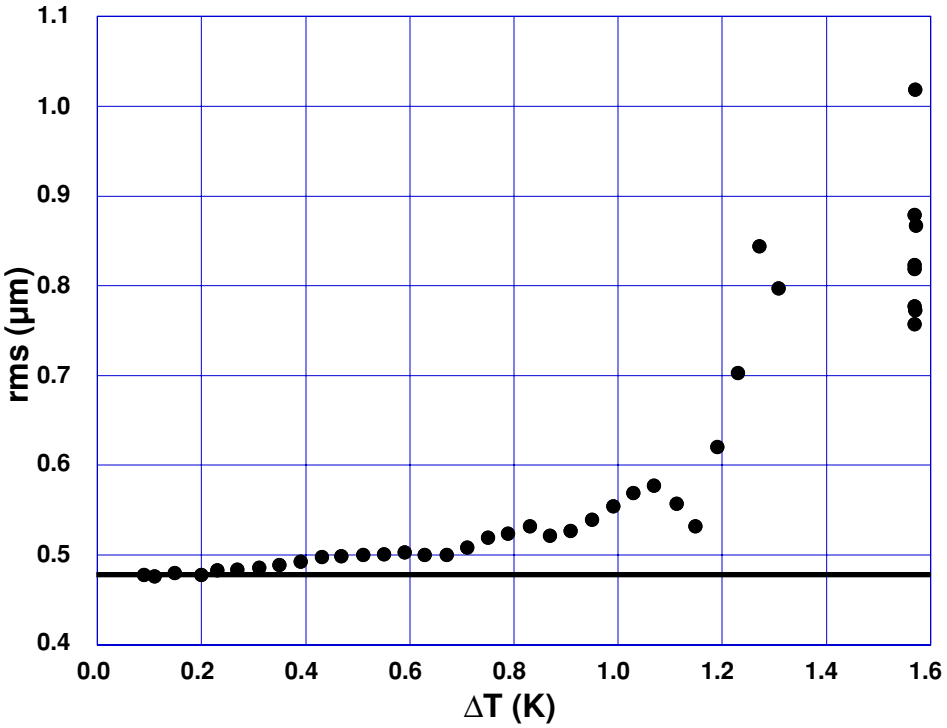

Generating Low Temperature Layers with IR Heating Figure 2

D.N. Bittner, G.W. Collins, and J.D. Sater

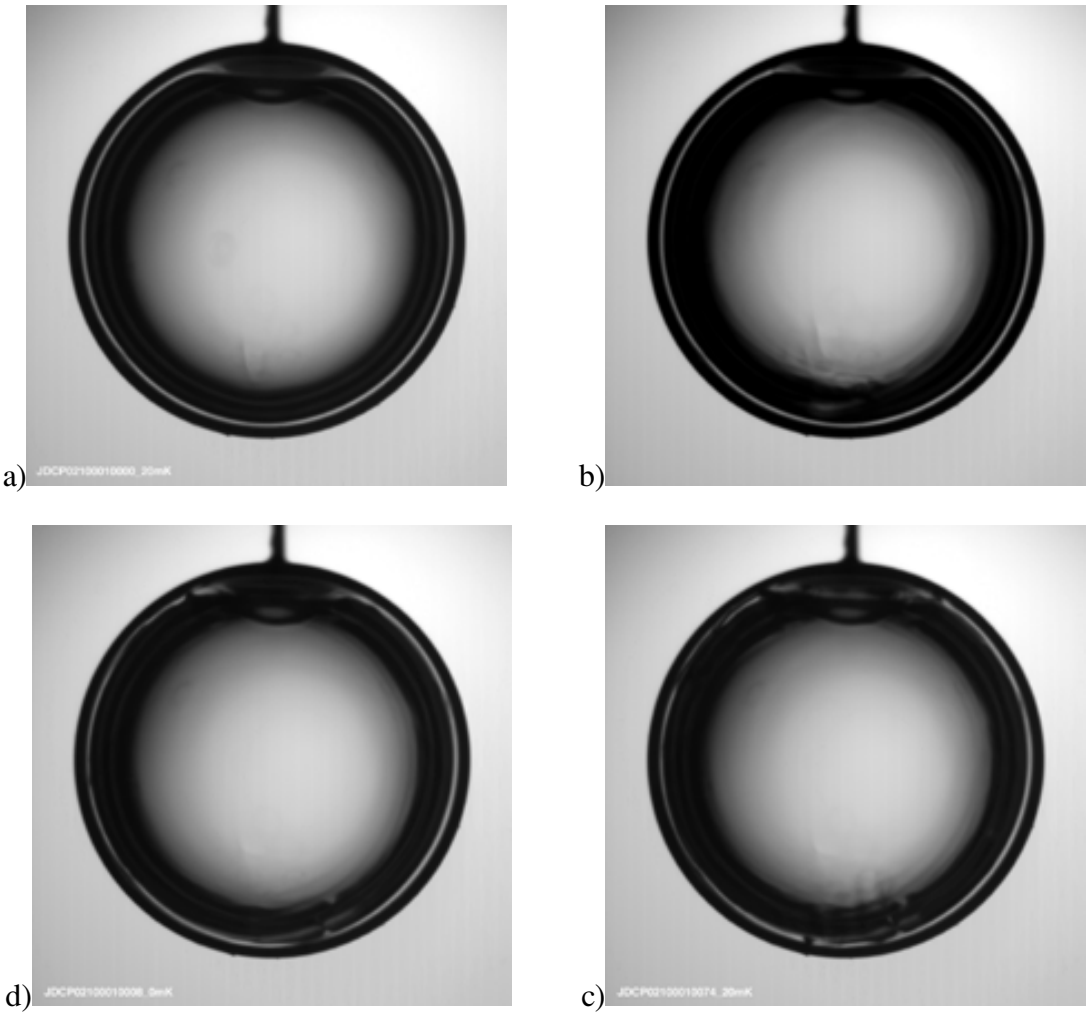

Generating Low Temperature Layers with IR Heating Figure 3

D.N. Bittner, G.W. Collins, and J.D. Sater

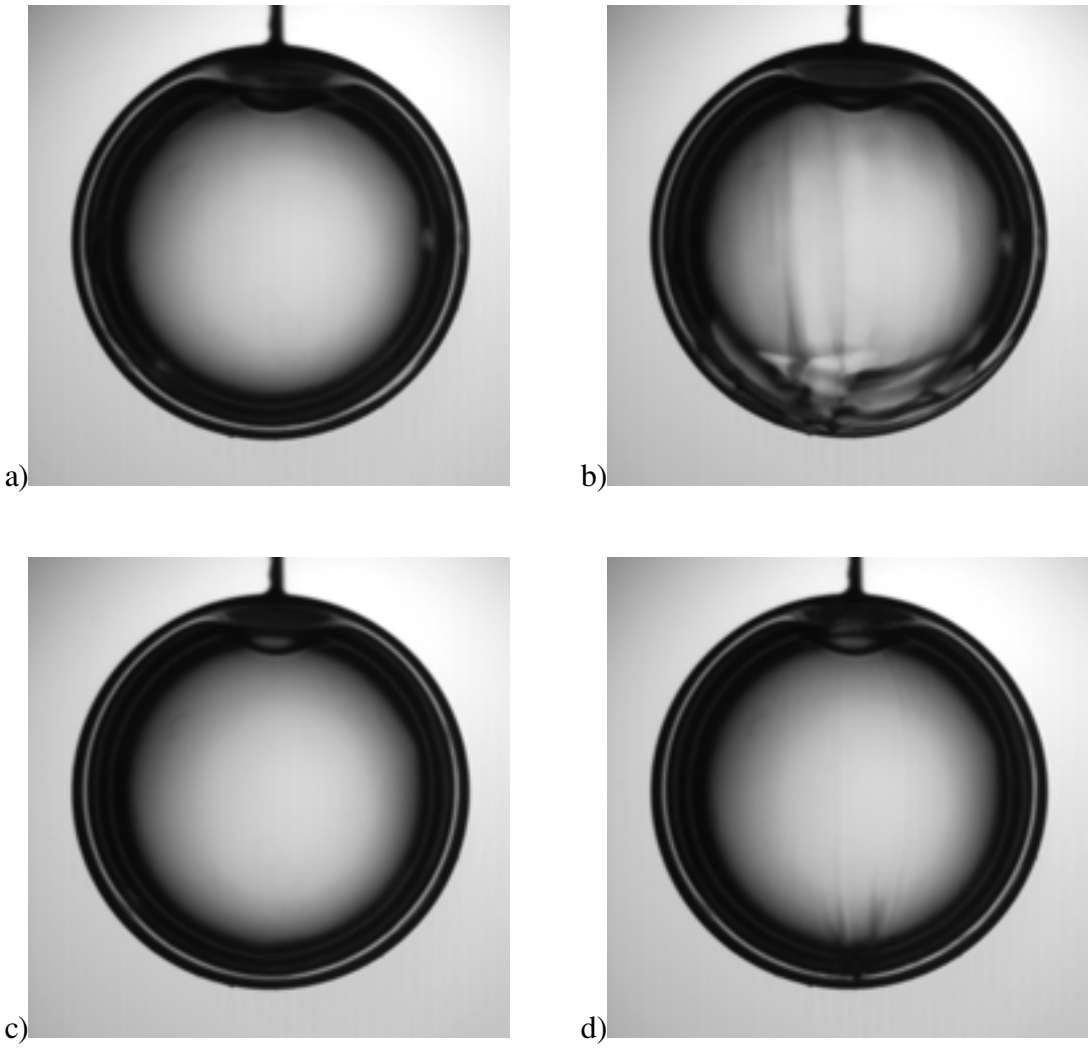

Generating Low Temperature Layers with IR Heating Figure 4

D.N. Bittner, G.W. Collins, and J.D. Sater

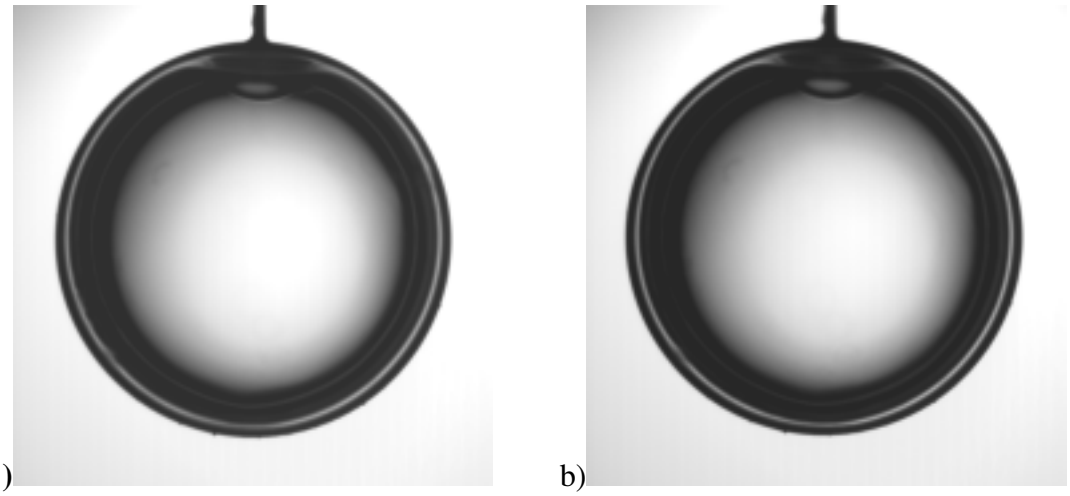

a) b)

Generating Low Temperature Layers with IR Heating Figure 5

D.N. Bittner, G.W. Collins, and J.D. Sater

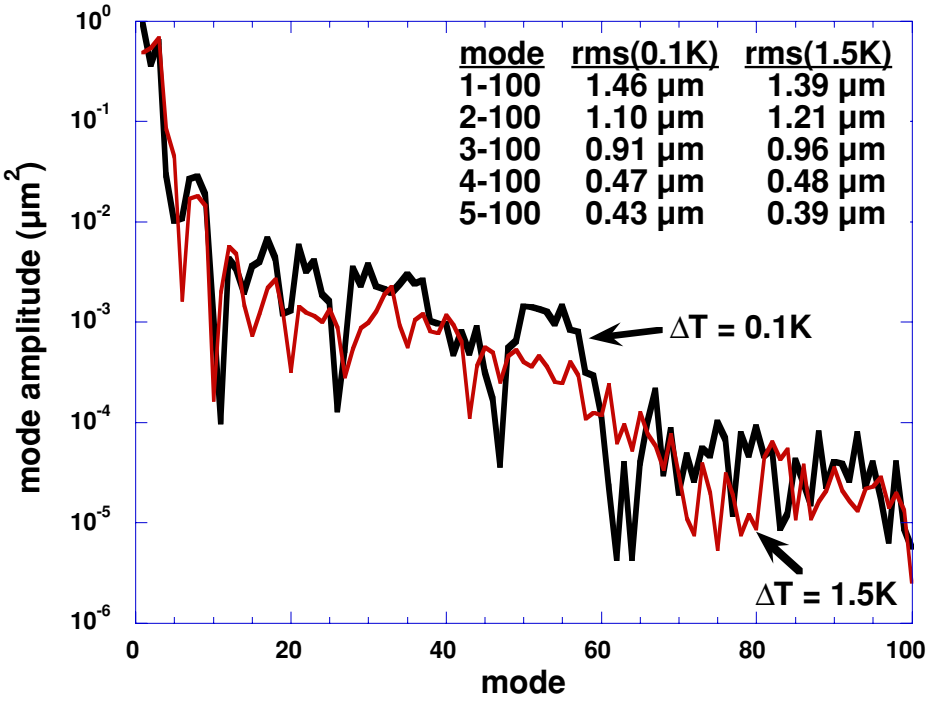

Generating Low Temperature Layers with IR Heating Figure 6

D.N. Bittner, G.W. Collins, and J.D. Sater